NRC Research Press

ARTICLE

Methods for evaluating the utilities of local and global maps for increasing the precision of estimates of subtropical forest area

Ronald E. McRoberts, Alexander C. Vibrans, Christophe Sannier, Erik Næsset, Matthew C. Hansen, Brian F. Walters, and Débora V. Lingner

Abstract: For a study area in the Brazilian state of Santa Catarina, the utilities of local and global forest maps in combination with poststratified and model-assisted estimators for increasing the precision of estimates of forest area were compared. Auxiliary information was in the form of local maps, the recent Global Forest Change map, and combinations of these maps. The poststratified estimators produced estimates of greater precision than the model-assisted regression estimators for maps of categorical variables, but the model assisted estimators produced estimates of greater precision for maps of continuous variables. The Global Forest Change map was the least accurate of all the maps, but it produced estimates of forest area that were similar to those for the other maps and that were more precise than if the map had not been used. Thus, the Global Forest Change map may be an attractive option if local maps are not available or cannot be constructed. The primary contributions of the study are two-fold. First, this is one of the first case studies that rigorously assess the utility of global maps for national estimation. After accumulation of a few more such studies, broader generalizations should be forthcoming. Second, a statistical basis is provided for the previously unexplained greater precision for poststratified estimators than for model-assisted estimators.

Key words: logistic regression model, inference, Santa Catarina, Brazil.

Résumé : Sur la base d'une zone d'étude située dans l'État de Santa Catarina au Brésil, nous avons comparé l'utilité de cartes du couvert forestier locales et mondiale combinées à des estimateurs stratifiés a posteriori ou assistés par un modèle pour augmenter la précision de l'estimation des superficies forestières. L'information auxiliaire était représentée par les cartes locales, la carte récemment produite de 'Global Forest Change' et différentes combinaisons de ces cartes. Pour les cartes à valeurs catégoriques, les estimateurs stratifiés a posteriori ont produit des estimations plus précises que les estimateurs assistés par un modèle de régression, mais, pour les cartes à valeurs continues, les estimateurs assistés par un modèle de régression ont produit des estimations de plus grande précision que les estimateurs stratifiés. La carte de 'Global Forest Change' était la moins précise de toutes les cartes mais elle a produit des estimations de la superficie forestière semblables à celles des autres cartes et plus précises que si seules les données de terrain avaient été utilisées. Par conséquent, la carte des changements du couvert forestier mondial peut être une option intéressante si les cartes locales ne sont pas disponibles ou ne peuvent être produites. Les principales contributions de cette étude résident en deux volets. Premièrement, il s'agit d'une des premières études de cas qui évalue rigoureusement l'utilité des cartes mondiales pour des estimations à l'échelle nationale. Après que d'autres études semblables auront été réalisées, il devrait être possible de généraliser ce fait plus largement. Deuxièmement, nous proposons des fondements statistiques qui permettent dorénavant d'expliquer la plus grande précision des estimateurs stratifiés comparativement aux estimateurs assistés par un modèle. [Traduit par la Rédaction]

Mots-clés : modèle de régression logistique, inférence, Santa Catarina, Brésil.

1. Introduction

1.1. Background

In the framework of the United Nations program, Reducing Emissions from Deforestation and Forest Degradation (REDD), incentive payments to developing countries for reducing forest-related greenhouse gas (GHG) emissions are results based, meaning that the payments are contingent on the countries providing convincing evidence that reduction targets have been achieved (Voigt and Ferreira 2015). In this framework, the evidence must be in the form of accurate and precise estimates of forest resources, particularly forest area. This requirement is recognized as a key component of monitoring, reporting, and verification programs implemented in tropical and subtropical countries under the auspices of the United National Framework Convention on Climate Change (UNFCCC). For example, estimation of forest area is a primary component of the gain–loss approach to carbon accounting recommended by the Intergovernmental Panel on Climate Change (IPCC) (Penman et al. 2003). Additional and extended guid-

Received 11 February 2016. Accepted 23 March 2016.

R.E. McRoberts and B.F. Walters. Northern Research Station, U.S. Forest Service, Saint Paul, Minnesota, MN, USA.
A.C. Vibrans and D.V. Lingner. Universidade Regional de Blumenau, Blumenau, Santa Catarina, Brazil.
C. Sannier. Systèmes d'Information à Référence Spatiale, Villeneuve d'Ascq, France.
E. Næsset. Department of Ecology and Natural Resource Management, Norwegian University of Life Sciences, Ås, Norway.
M.C. Hansen. Department of Geographical Sciences, University of Maryland, College Park, MD, USA.
Corresponding author: Ronald E. McRoberts (email: rmcroberts@fs.fed.us).

This work is free of all copyright and may be freely built upon, enhanced, and reused for any lawful purpose without restriction under copyright or database law. The work is made available under the Creative Commons CC0 1.0 Universal Public Domain Dedication (CC0 1.0).

Published at www.nrcresearchpress.com/cjfr on 30 May 2016.

ance is provided by the Methods and Guidance document (Global Forest Observations Initiative (GFOI) 2013) and the associated module on using global tree cover and change datasets (GFOI 2015). With the gain–loss approach, the net balance of additions to and removals from a carbon pool is estimated as the product of the area of land use change, called activity data, and the responses of carbon stocks for particular land use change categories on a per unit area basis, called emission factors. For these GHG inventories, the IPCC defines two good practice criteria: (*i*) "neither over- nor under-estimates as far as can be judged", and (*ii*) "uncertainties are reduced as far as practicable" (see preface in Penman et al. (2003)); in this context, uncertainty is conceptually equivalent to the inverse of precision. Thus, the importance of not only the accuracy, but also the precision, of estimates of forest area must be emphasized.

Satisfaction of precision criteria for estimates of forest area is difficult to achieve apart from augmenting the estimation process with auxiliary information. One effective approach has been to use stratified estimators, whereby auxiliary information in the form of classifications of satellite spectral data serve as the basis for strata. Two sets of stratified estimators are distinguished. First, when strata are defined before sampling and within-strata sample sizes are selected in advance, the term stratified is used to characterize the estimators, whereas when the sample is selected without regard to the strata and the within-strata sample sizes are random, the term poststratified (PSTR) is used to characterize the estimators. The Forest Inventory and Analysis program of the U.S. Forest Service, which conducts the national forest inventory of the United States of America, has devoted considerable effort to investigating PSTR estimators using satellite spectral data; much of this research is summarized in McRoberts et al. (2005) and Westfall et al. (2011). Stratified estimators are also increasingly used for estimating tropical forest area. Tyukavina et al. (2013) used stratified estimators and Landsat data to estimate forest area for the Democratic Republic of the Congo, and Potapov et al. (2014) used stratified estimators and Landsat data to estimate the extent of forest cover in Peru. Olofsson et al. (2013, 2014) illustrated stratified estimators using information in a confusion matrix and provided corresponding good practice guidelines. The general conclusion from these and similar studies is that both stratified and PSTR estimators with remote sensing based strata have the potential to reduce the variances of estimates of forest area by factors of three or greater relative to the variances of estimates obtained using only plot data.

Recently, model-assisted regression estimators have been used with remotely sensed auxiliary information to increase the precision of estimates of parameters related to forest area. McRoberts (2011) used Landsat data and model-assisted estimators to estimate areas of forest, nonforest, coniferous forest, and deciduous forest, and McRoberts (2014) extended these techniques to estimate areas of afforestation, deforestation, and net deforestation. Vibrans et al. (2013) used model-assisted estimators with forest inventory data and remote sensing based land cover maps to estimate forest area for Santa Catarina, Brazil. Sannier et al. (2014, 2016) estimated forest area change for Gabon using model-assisted estimators and maps based on Landsat data. These techniques have been highly effective, with the variances of estimates of forest area reduced by factors as great as 30 and variances of estimates of forest area change reduced by factors as great as 3.5 relative to variances of simple random sampling (SRS) estimates (Sannier et al. 2016).

Only a few comparisons of model-assisted estimators and either form of stratified estimators have been reported. Stehman (2009) demonstrated that PSTR and model-assisted estimators are closely related and can be encompassed within the same inferential framework. For continuous response variables, McRoberts et al. (2013) and Sannier et al. (2014) reported that model-assisted estimators produced greater precision than PSTR estimators. However, for categorical response variables, Stehman (2013) reported that stratified estimators produced comparable or greater precision than model-assisted regression estimators when the stratification variable and the inventory response variable were the same. McRoberts et al. (2014) reported similar results for PSTR estimators.

Construction of remote sensing based land cover maps typically entails acquisition of the remotely sensed data, training data to guide classification or prediction, and reference data for assessing accuracy. These tasks can be costly, laborious, and time consuming. Therefore, use of local existing maps can be an efficient alternative (McRoberts et al. 2002; Vibrans et al. 2013). Although the usual challenge is that few, if any, relevant maps are available, on occasion, the challenge may be to choose from among multiple maps. For example, for the Brazilian State of Santa Catarina, Vibrans et al. (2013) reported comparisons of four land cover maps that were aggregated to forest–nonforest. Although model-assisted estimates and their variances were similar for several of the maps, they all exhibited deficiencies for particular applications. An alternative approach that merits consideration is to combine maps in such a way that the resulting map capitalizes on the relative strengths of the underlying maps while circumventing their deficiencies.

If no current local maps exist and the construction of maps is not feasible, then a third alternative is to use one of the existing continental or global forest cover and (or) forest cover change maps. The recently released Landsat based, Global Forest Change (GFC) map products at 30 m × 30 m resolution (Hansen et al. 2013) are one possibility. Other possibilities include the 30 m × 30 m Global Land Cover dataset based on Landsat and Huan Jing (Environment)-1 data (Jun et al. 2014). This dataset depicts 10 main land cover types for two reference years, 2000 and 2010. A third possibility is the global forest–nonforest map that is based on data from the Advance Land Observation Satellite, Phased Array type L-band Synthetic Aperture Radar, and depicts forest cover in four density classes for years between 2007 and 2010 (Shimada et al. 2014). The choice of a particular map depends on multiple factors, including the degree to which the maps and local reference data match with respect to factors such as dates, resolutions, and definitions.

1.2. Objectives

For a study area in the Brazilian State of Santa Catarina, the objectives were two-fold: (*i*) to compare estimates of proportion forest area and corresponding estimates of precision using a variety of local and global maps as auxiliary information, and (*ii*) to compare SRS, PSTR estimators, and model-assisted estimators with respect to the precision of estimates of proportion forest area.

2. Data

2.1. Study area

The study area was a 150 km × 150 km region in the east–central portion of the Brazilian state of Santa Catarina (Fig. 1). Santa Catarina includes dense ombrophylous forests and mixed ombrophylous forests with Araucaria phytogeographic subdivisions, as established by Klein (1978) and Veloso et al. (1991).

2.2. Forest and Floristic Inventory of Santa Catarina

Data from the Forest and Floristic Inventory of Santa Catarina (IFFSC) for the study area included ground plot observations of forest cover, structure, and composition obtained between 2007 and 2010 for a sample consisting of 255 plots located at the intersections of a 10 km × 10 km grid with a randomly selected starting position. This sampling design features sampling without replacement, with all potential plot centers having equal probabilities of inclusion into the sample. Sample plots consisted of clusters of four crosswise 1000 m² subplots (20 m × 50 m) and were used to collect field data (Vibrans et al. 2010). Plot centers were determined in the field using global positioning system receivers with a mean error of 4.1 m. For this study, assessments of only the northernmost subplot of each plot were used as a means of circumventing issues related to spatial correlation among observations for subplots of the same plot.

Fig. 1. Study area in the State of Santa Catarina, Brazil.

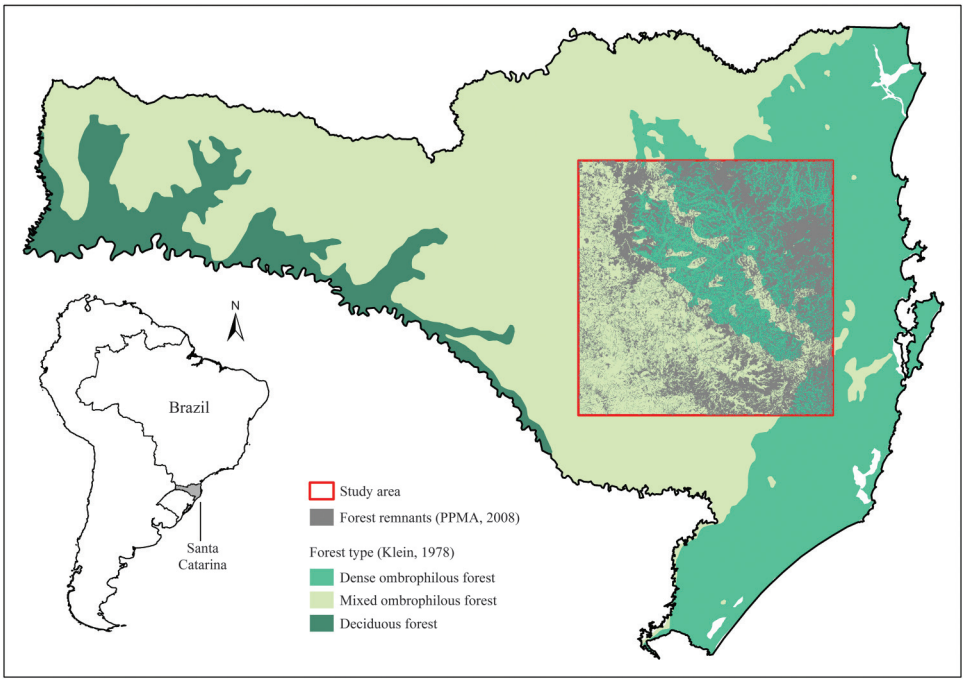

The forest–nonforest status of the plots was determined using the IFFSC definition of forest, which specifies woody vegetation with minimum area of 0.5 ha, canopy height of at least 10 m, and basal area of at least 10 $m^2 \cdot ha^{-1}$ (Vibrans et al. 2013). A nominal 10% canopy cover criterion was used, but cover of exactly 10% was difficult to assess in the field. However, subsequent analyses indicated that the height and basal area criteria produced canopy covers of at least 10%.

2.3. Local Santa Catarina maps

Four satellite image based land cover maps had previously been constructed for Santa Catarina: (*i*) a survey of forest remnants of Santa Catarina (Levantamento da Cobertura Florestal da Secretaria de Agricultura) designated LCF/SAR (SAR 2005); (*ii*) a survey of the native vegetation of the Atlantic forest designated PROBIO (Cruz and Vincens 2007); (*iii*) an atlas of the Atlantic forest remnants designated Atlas 2008 (Fundação SOS Mata Atlântica 2009); and (*iv*) a general thematic map of the state of Santa Catarina (Projeto de Proteção da Mata Atlântica) designated PPMA (Geoambiente Sensoriamento Remoto Ltda. 2008). Data for the four surveys and the resulting maps were kindly provided by the responsible institutions (Table 1). Vibrans et al. (2013) discussed the individual thematic classes for the four maps and how they were aggregated to the two classes, i.e., forest and nonforest.

2.4. GFC map

Of the previously referenced global datasets, the GFC data are most compatible with the local inventory data with respect to dates, resolution, and forest definition. The Landsat-based GFC map was acquired, clipped to the study area boundaries, and georectified with the inventory plot locations and local maps using a common coordinate system. The GFC year 2010 tree cover data are per pixel estimates of percent maximum tree canopy cover based on cloud-free, annual growing season, composite, Landsat 7 Enhanced Thematic Mapper Plus data. A regression tree model was used with annual composites from 2000 to 2012 inclusive (Hansen et al. 2013). Data gaps and noise were replaced using multiyear median values. The resulting layer represents estimated maximum percent tree canopy cover per 30 m × 30 m pixel in the range 1%–100% for vegetation taller than 5 m for the year 2010. For this study, the tree cover percentages were divided by 100 to convert them to proportions.

3. Methods

3.1. Combining maps

Two additional maps were constructed by combining information from the four local maps and the GFC map using a logistic regression model. The relationship between a Bernoulli response variable, $\boldsymbol{Y}$, such as forest–nonforest and a vector, $\boldsymbol{X}$, of predictor variables, whether categorical or continuous, is often expressed as

$$(1) \qquad \begin{aligned} p_i &= E(y_i) \\ &= f(\boldsymbol{X}_i;\ \boldsymbol{\beta}) \end{aligned}$$

where i indexes population units, $E(.)$ denotes statistical expectation, p_i is the probability that $y_i = 1$, and $\boldsymbol{\beta}$ is a vector of parameters to be estimated (Agresti 2007). The function $f(\boldsymbol{X}_i;\ \boldsymbol{\beta})$ expresses the statistical expectation of $\boldsymbol{Y}$ in terms of $\boldsymbol{X}$ and $\boldsymbol{\beta}$ and is often formulated using the logistic function as

$$(2) \qquad f(\boldsymbol{X}_i;\ \boldsymbol{\beta}) = \frac{\exp\left(\boldsymbol{\beta}_0 + \sum_{j=1}^{J} \boldsymbol{\beta}_j x_{ij}\right)}{1 + \exp\left(\boldsymbol{\beta}_0 + \sum_{j=1}^{J} \boldsymbol{\beta}_j x_{ij}\right)}$$

where exp(.) is the exponential function. For this study, j indexes maps, and $\boldsymbol{Y}$ is forest–nonforest, with $y_i = 0$ denoting nonforest and $y_i = 1$ denoting forest. The model parameter vector, $\boldsymbol{\beta}$, was estimated using the maximum likelihood method (Agresti 2007).

The logistic regression model was fit using the IFFSC forest–nonforest observations as the response variable and the forest–nonforest data from the four local maps as the predictor variables. The model of eq. 2 with estimated parameter values was then used to predict the probability of forest for each pixel with the result designated the SC map because it is based on the combination of

Table 1. Attributes of Santa Catarina land cover maps.

Map attribute	Map			
	LCF/SAR (2005)	PROBIO (2007)	Atlas 2008 (2009)	PPMA (2010)
Executor	State Secretary of Agriculture	Federal Ministry of Environment	NGO	State Environment Agency
Satellite, sensor (year of image capturing)	Landsat-5 TM, Landsat-7 ETM+ (2003 and 2004)	Landat-7 ETM+ (2001–2003), SRTM (2000)	CBERS-2 CCD (2005), Landsat-5 TM (2005–2008)	SPOT-4 (2005)
Scale of classification/presentation	1:50 000/1:50 000	1:250 000/1:250 000	1:50 000/1:50 000	1:50 000/1:50 000
Spatial resolution	30 m × 30 m	30 m × 30 m	30 m × 30 m	20 m × 20 m (10 m × 10 m pan)
Minimal mapping area (nominal)	10 ha	40 ha	5 ha	2.5 ha
Definition of forest	Forests (mangrove and restinga excluded)	Forests of three types: DEN, MIX, DEC and ecotons (mangrove and restinga excluded)	Primary and secondary forest formations (mangrove and restinga excluded)	Primary forests and forests at medium and advanced successional stages (no initial successional stage forests)

the four Santa Catarina maps. Similarly, the logistic regression model was fit using the IFFSC forest–nonforest observations as the response variable and both the forest–nonforest data from the four local maps and the GFC tree cover proportions as the predictor variables. The model of eq. 2 with the estimated parameter values was then used to predict the probability of forest for each pixel, with the result designated the SC+GFC map.

3.2. Constructing forest–nonforest maps

The GFC map consists of continuous tree cover proportions in the range [0, 1], and the SC and SC+GFC maps consist of continuous probabilities of forest, also in the range [0, 1]. The continuous values for all three maps were used with multiple threshold (T) values to construct forest–nonforest maps. For the GFC map, if the proportion tree cover for a pixel exceeded T, then the pixel was classified as forest; otherwise, the pixel was classified as nonforest. For the SC and SC+GFC maps, if the probability of forest from eq. 2 exceeded T, then the pixel was classified as forest; otherwise, the pixel was classified as nonforest. The following three thresholds were used: $T = 0.1$, $T = 0.3$, and $T = 0.5$. The first threshold corresponds to the minimum canopy cover for the IFFSC definition of forest and is also the minimum value recommended by the UNFCCC (2006); the second threshold is the maximum value recommended by the UNFCCC; and the third threshold is commonly used to distinguish classes when using logistic model predictions. In summary, 16 maps were available: four local forest–nonforest maps; nine additional forest–nonforest maps constructed using each of the three thresholds with each of the SC, GFC, and SC+GFC maps; the GFC proportion tree cover map; and the SC and SC+GFC probability of forest maps.

3.3. Map accuracy

The accuracies of the 13 forest–nonforest maps were evaluated using error matrices, where overall accuracy (OA) is the proportion of observations correctly classified, user's accuracy (UA) is the ratio of the number of correct classifications and the total number of predictions for a class, and producer's accuracy (PA) is the ratio of the number of correct classifications and the total number of observations for a class.

3.4. Inference

Because forest area is simply the product of total area and proportion forest area and because total area is known, estimation focused on proportion forest area. The ultimate inferential objective was to construct confidence intervals for estimates of proportion forest area for the entire study area. These intervals are expressed as

$$\hat{\mu} \pm t\,\mathrm{SE}(\hat{\mu}) \tag{3}$$

where $\hat{\mu}$ is the estimate of proportion forest area, $\mathrm{SE}(\hat{\mu}) = \sqrt{\hat{\mathrm{Var}}(\hat{\mu})}$ is the standard error of $\hat{\mu}$, and the factor t depends on the desired significance level and the distribution of the response variable. For most distributions and applications, $t = 2$ produces an approximate 95% confidence interval. For purposes of constructing confidence intervals, the focus of the study was estimation of mean proportion forest area and the variance and SE of the estimated mean using SRS, PSTR, and model-assisted estimators. In the probability-based or design-based frameworks, all three estimators are unbiased or asymptotically unbiased in the sense that the mean of estimates obtained using the estimator over all possible samples equals the true value. However, the estimate obtained with any particular sample may deviate substantially from the true value, hence the relevance of confidence intervals.

3.4.1. SRS estimators

Proportion forest area was estimated using only the observations from the IFFSC ground sample under the assumption of SRS.

For an equal probability sample, the SRS estimator of proportion forest, $\hat{\mu}_{SRS}$, is simply the proportion of sample plots classified as forest cover

$$\hat{\mu}_{SRS} = \frac{1}{n}\sum_{i=1}^{n} y_i \tag{4}$$

where n is the sample size, i indexes the sample units, and

$$y_i = \begin{cases} 0 & \text{if nonforest land cover is observed} \\ 1 & \text{if forest land cover is observed} \end{cases} \tag{5}$$

For the Bernoulli variable defined by eq. 5, an estimator of the variance of $\hat{\mu}_{SRS}$ is

$$\begin{aligned} \hat{\text{Var}}(\hat{\mu}_{SRS}) &= \frac{1}{n(n-1)}\sum_{i=1}^{n}(y_i - \hat{\mu}_{SRS})^2 \\ &= \frac{\hat{\mu}_{SRS}(1-\hat{\mu}_{SRS})}{n(n-1)} \end{aligned} \tag{6}$$

When a systematic sample is used, as for this study, variances may be overestimated relative to estimates based on a simple random sample (Särndal et al. 1992, p. 83), although Aune-Lundberg and Strand (2014) note that the SRS estimators are still safe and conservative. The primary advantages of the SRS estimators are that they are intuitive and unbiased, but the disadvantage is that variances may be large, particularly for small sample sizes and (or) highly variable populations.

3.4.2. PSTR estimators

The essence of stratification is to disaggregate the population into a small number of homogenous classes or strata and then calculate the population mean as a weighted mean of the within-stratum means, where the weights are proportional to the strata sizes. For appropriate strata, stratification can reduce the variances of estimates of the population mean relative to variances obtained using the SRS estimators. Use of stratified estimators requires accomplishment of two tasks: (*i*) calculation of the strata weights and (*ii*) assignment of each sample unit to a single stratum. The first task is accomplished by calculating the strata weights as proportions of population units in strata. The second task was accomplished for this study by assigning the IFFSC plots to strata on the basis of the strata assignments of the map units containing the plot centers.

Forest inventory and monitoring programs increasingly use permanent plots whose locations are based on systematic grids and sampling intensities that are constant over large geographic areas. In such cases, stratified sampling is not possible, but precision may still be increased by using PSTR estimators subsequent to the sampling. PSTR estimates of means and variances are calculated using estimators provided by Cochran (1977)

$$\hat{\mu}_{PSTR} = \sum_{h=1}^{H} w_h \hat{\mu}_h \tag{7}$$

where

$$\hat{\mu}_h = \frac{1}{n_h}\sum_{i=1}^{n_h} y_{hi} \tag{8}$$

and where $h = 1, \ldots, H$ denotes strata, y_{hi} is the ith sample observation in the hth stratum, w_h is the weight for the hth stratum, n_h is the number of plots assigned to the hth stratum, and $\hat{\mu}_h$ is the sample estimate of the within-stratum mean. For poststratification, Cochran (1977, p. 135) provides an estimator of the variance

$$\hat{\text{Var}}(\hat{\mu}_{PSTR}) = \sum_{h=1}^{H}\left[w_h\frac{\hat{\sigma}_h^2}{n} + (1-w_h)\frac{\hat{\sigma}_h^2}{n^2}\right] \tag{9}$$

where

$$\hat{\sigma}_h^2 = \frac{1}{n_h - 1}\sum_{i=1}^{n_h}(y_{hi} - \hat{\mu}_h)^2 \tag{10}$$

The utility of a stratification for increasing the precision of estimates is often assessed using relative efficiency (RE), which, for this study, was defined as

$$\text{RE} = \frac{\hat{\text{Var}}(\hat{\mu}_{SRS})}{\hat{\text{Var}}(\hat{\mu}_{PSTR})} \tag{11}$$

where RE > 1.0 indicates a reduction in variance and an increase in precision.

Strata were constructed using two approaches. First, for each of the 13 forest–nonforest maps, the forest–nonforest classes were used as strata. Second, for the SC, GFC, and SC+GFC maps, strata boundaries for separating the forest and nonforest strata were selected to minimize the PSTR variance estimate from eq. 9 by considering all possible boundaries between 0.01 and 0.99 in increments of 0.01. Map accuracy assessments, as described in Section 3.2, were also conducted for forest–nonforest maps for which the latter optimal thresholds were used to distinguish the classes. Of importance, map inaccuracy does not contribute to bias in the estimator but only causes the variance of the stratified estimate to increase and the RE to decrease (Gregoire and Valentine 2008, section 5.5).

Concerns may be raised regarding the validity of estimates obtained using stratifications constructed using the same sample observations as are used to calculate estimates. Breidt and Opsomer (2008) demonstrated that when strata are constructed by dividing the range of predictions obtained from a regression model calibrated using the response variable observations, the detrimental effects of violating the stratification assumptions are negligible, even for small sample sizes. Dahlke et al. (2013) and Tipton et al. (2013) extended these results to include nonparametric prediction procedures.

3.3.3. Model-assisted estimators

Model-assisted regression estimators use models based on auxiliary data to enhance inferences but rely on the probability sample for validity (Särndal et al. 1992). An initial estimator of proportion forest area based only on the map data, designated the synthetic estimator ($\hat{\mu}_{Syn}$), is formulated as

$$\hat{\mu}_{Syn} = \frac{1}{N}\sum_{i=1}^{N}\hat{y}_i \tag{12}$$

where N is the population size and $\hat{y}_i$ is the map prediction. For forest–nonforest maps, $\hat{y}_i = 0$ if the map class is nonforest and $\hat{y}_i = 1$ if the map class is forest; for the GFC map, $\hat{y}_i$ takes on the continuous values of proportion tree cover; and for the SC and SC+GFC maps, $\hat{y}_i$ takes on the continuous values of the probability

of forest. Systematic map classification and prediction errors induce bias into this estimator, which can be estimated as follows:

$$\hat{\text{Bias}}(\hat{\mu}_{\text{Syn}}) = \frac{1}{n}\sum_{i=1}^{n}\varepsilon_i \tag{13}$$

where $\varepsilon_i = \hat{y}_i - y_i$. The model-assisted, generalized regression (GREG) estimator is then defined as

$$\begin{aligned}\hat{\mu}_{\text{GREG}} &= \hat{\mu}_{\text{Syn}} - \hat{\text{Bias}}(\hat{\mu}_{\text{Syn}}) \\ &= \frac{1}{N}\sum_{i=1}^{N}\hat{y}_i - \frac{1}{n}\sum_{i=1}^{n}\varepsilon_i\end{aligned} \tag{14}$$

with variance estimator

$$\hat{\text{Var}}(\hat{\mu}_{\text{GREG}}) = \frac{1}{n(n-1)}\sum_{i=1}^{n}(\varepsilon_i - \bar{\varepsilon})^2 \tag{15}$$

where $\bar{\varepsilon} = \frac{1}{n}\sum_{i=1}^{n}\varepsilon_i$ (Särndal et al. 1992, section 6.5; Särndal 2011). Of importance, correction for estimated bias compensates for map inaccuracy, making the GREG estimator asymptotically unbiased. RE was calculated as

$$\text{RE} = \frac{\hat{\text{Var}}(\hat{\mu}_{\text{SRS}})}{\hat{\text{Var}}(\hat{\mu}_{\text{GREG}})} \tag{16}$$

The primary advantage of the GREG estimators is that they capitalize on the relationship between the sample observations and their model predictions in the form of map data to reduce the variance of the estimate of the population mean.

4. Results and discussion

4.1. Map accuracies

Absolute values for estimates of the logistic regression model parameters were greatest for the PPMA map, which had the greatest OA of the four original maps, and smallest for the LCF/SAR maps, which had the smallest OA of the four original maps. Thus, predictions for maps constructed using the logistic regression model and information from the four original maps were most influenced by the most accurate original map and least influenced by the least accurate original map.

For the four local maps, OAs ranged from 0.75 to 0.82; for the four forest–nonforest maps derived from the SC map, which consists of probabilities of forest, all OAs were 0.82; for the four forest–nonforest maps derived from the GFC proportion tree cover map, OAs ranged from 0.62 to 0.69; and for the four forest–nonforest maps derived from the SC+GFC probability of forest map, OAs ranged from 0.63 to 0.83 (Table 2). Thus, considering all OAs, the forest–nonforest maps derived from the SC probability of forest map were the most accurate overall, followed by the four local maps, then the forest–nonforest maps derived from the SC+GFC probability of forest map, and finally, the forest–nonforest maps derived from the GFC proportion tree cover maps.

Several map accuracy issues are worth noting. First, maps derived from the SC probability of forest map were as accurate, or more accurate, than the four local maps. Second, when considering OA, PA, and UA together, maps derived from the SC probability of forest map were consistently more accurate across all measures than any of the other maps, although the PPMA map was only slightly less accurate. Third, use of the proportion tree cover data from the GFC map as a predictor variable when constructing the SC+GFC map led to a slight loss of accuracy in the derived forest–nonforest maps relative to the maps derived from the SC map. Finally, greater values of the threshold, T, generally produced greater accuracies.

Table 2. Map accuracies.

		Accuracies				
			PA		UA	
Map	Threshold (T)	OA	Nonforest	Forest	Nonforest	Forest
Atlas 2008	—	0.76	0.71	0.56	0.92	0.86
LCF/SAR	—	0.75	0.74	0.69	0.79	0.75
PPMA	—	0.82	0.84	0.84	0.80	0.79
PROBIO	—	0.75	0.72	0.65	0.84	0.78
SC	0.10*	—	—	—	—	—
	0.30	0.82	0.85	0.84	0.79	0.76
	0.50	0.82	0.85	0.84	0.80	0.79
	0.50†	0.82	0.85	0.84	0.80	0.79
GFC	0.10	0.62	0.88	0.95	0.33	0.56
	0.30	0.64	0.87	0.94	0.36	0.57
	0.50	0.66	0.87	0.93	0.41	0.59
	0.95†	0.69	0.76	0.79	0.61	0.65
SC+GFC	0.10	0.63	0.92	0.97	0.32	0.56
	0.30	0.79	0.85	0.85	0.74	0.75
	0.50	0.82	0.84	0.83	0.82	0.81
	0.57†	0.83	0.84	0.83	0.83	0.81

Note: OA, overall accuracy; PA, producer's accuracy; UA, user's accuracy; SC, combination of the four local Santa Catarina maps; GFC, Global Forest Change map; SC+GFC, combination of the four local Santa Catarina maps and the Global Forest Change map.

*All plots had predicted probabilities of forest greater than the threshold.

†Threshold value that maximized OA and minimized the poststratified estimate of standard error.

Values of the threshold, T, for the GFC-derived forest–nonforest maps had little effect on OAs. Within the small range of values, the least accurate map was produced using $T = 0.10$, which corresponds most closely to the nominal 10% canopy cover used by the IFFSC and is also the minimum value recommended by the UNFCCC, and the second least accurate map was produced using $T = 0.30$, which corresponds to the maximum value recommended by the UNFCCC. For the GFC map, OA was maximized for $T = 0.95$ (Table 2). For a related study in Gabon, Sannier et al. (2016) found that a threshold of $T = 0.70$ for the GFC map produced the greatest accuracy.

4.2. SRS estimators

The SRS estimators that use only the IFFSC plot-level forest–nonforest observations produced $\hat{\mu}_{\text{SRS}} = 0.475$ and $\text{SE}(\hat{\mu}_{\text{SRS}}) = 0.031$. Because use of the SRS variance estimator with data obtained from a systematic sample may be positively biased, additional variance estimators could be considered. For this study, a variance estimator proposed by Wolter (1984) to accommodate this issue produced variance estimates that deviated proportionally by less then 0.01 from estimates obtained using the SRS variance estimator. This result confirms the conclusion of Aune-Lundberg and Strand (2014) that the SRS estimators are "a safe and conservative alternative when spatial autocorrelation is absent or unknown". Therefore, for this study, estimates obtained using the SRS estimators are used for comparison purposes. In particular, when the sample is proportionally allocated to strata, as is the sample for this study, the SRS and PSTR estimates of the mean converge asymptotically as the sample size increases.

4.3. PSTR estimators

As expected, the unbiased PSTR estimators produced similar estimates of proportion forest area ranging from 0.429 to 0.471, regardless of the map used as auxiliary information (Table 3). Although the overall range of SEs was also small (0.024 to 0.030), the forest–nonforest maps derived from the SC probability of for-

Table 3. Estimates of proportion forest.

	PSTR estimates				Model-assisted estimates					
Map	Threshold (T)	$\hat{\mu}_{PSTR}$	SE($\hat{\mu}_{PSTR}$)	RE	Threshold (T)	$\hat{\mu}_{Syn}$	$\hat{\text{Bias}}(\hat{\mu}_{Syn})$	$\hat{\mu}_{GREG}$	SE($\hat{\mu}_{GREG}$)	RE
Atlas 2008	—	0.454	0.027	1.311	—	0.282	−0.157	0.439	0.029	1.141
LCF/SAR	—	0.469	0.028	1.285	—	0.428	−0.035	0.463	0.032	0.983
PPMA	—	0.437	0.024	1.655	—	0.443	0.027	0.416	0.027	1.358
PROBIO	—	0.453	0.028	1.263	—	0.348	−0.082	0.431	0.031	1.005
SC	10*	—	—	—	0.10	1.000	0.525	0.475	0.031	1.000
	30	0.444	0.024	1.665	0.30	0.462	0.035	0.426	0.027	1.362
	50	0.438	0.024	1.690	0.50	0.449	0.031	0.418	0.027	1.390
	50†	0.438	0.024	1.690	Continuous	0.436	0.000	0.436	0.024	1.774
GFC	10	0.463	0.030	1.127	0.10	0.777	0.329	0.448	0.032	0.931
	30	0.461	0.029	1.150	0.30	0.753	0.310	0.443	0.033	0.928
	50	0.453	0.028	1.214	0.50	0.706	0.278	0.428	0.032	0.946
	95†	0.471	0.027	1.374	Continuous	0.682	0.246	0.436	0.030	1.082
SC+GFC	10	0.460	0.029	1.168	0.10	0.785	0.341	0.444	0.032	0.973
	30	0.443	0.025	1.551	0.30	0.488	0.067	0.421	0.028	1.226
	50	0.436	0.024	1.691	0.50	0.433	0.012	0.414	0.026	1.414
	57†	0.429	0.024	1.737	Continuous	0.433	0.000	0.433	0.023	1.830

Note: SC, combination of four local Santa Catarina maps; GFC, Global Forest Change map; SC+GFC, combination of four local Santa Catarina maps and the Global Forest Change map; PSTR, poststratified; Syn, synthetic; GREG, generalized regression; RE, relative efficiency.

*All plots had predicted probabilities of forest greater than the threshold.

†Threshold value that maximized the overall accuracy and minimized the PSTR estimate of standard error.

est map produced the smallest SEs, whereas the forest–nonforest maps derived from the GFC proportion tree cover map produced the largest SEs. Optimal values for the thresholds, T, that separated the nonforest and forest strata were proportion tree cover of 0.95 for the GFC map, probability of forest of 0.50 for the SC map, and probability of forest of 0.57 for the SC+GFC map (Table 3). Despite producing the least accuracies and greatest SEs, the four forest–nonforest maps derived from the GFC proportion tree cover map all produced RE values > 1.0 for all threshold values, meaning that the combination of the GFC-derived forest–nonforest maps and the PSTR estimators produced greater precision than the SRS estimators, which used no auxiliary information.

4.4. Model-assisted estimators

The asymptotically unbiased model-assisted GREG estimators also produced similar estimates of mean proportion forest area that ranged from 0.414 to 0.475 (Table 3). Although the synthetic estimates of mean proportion forest area deviated greatly, ranging from 0.282 to 1.000, the GREG adjustments for estimated bias compensated for the deviations. The GFC proportion tree cover map and the three forest–nonforest maps obtained using the thresholds of T = 0.10, T = 0.30, and T = 0.50 all produced RE values < 1.0, meaning that the SRS estimators that did not use map data as auxiliary information produced greater precision than the GREG estimators. Overall, SEs were smallest and REs were greatest when using the continuous probability of forest map data for the SC and SC+GFC maps. Finally, adjustments for estimated bias were greater for smaller threshold values.

4.5. PSTR versus model-assisted estimators

When using the categorical, forest–nonforest map data, the PSTR estimators consistently produced smaller SEs and larger REs than the GREG estimators (Table 3). This result confirmed the previous findings of Stehman (2013) and McRoberts et al. (2014) that when the classes of a categorical response variable correspond to the strata, stratified estimators produce greater precision than model-assisted estimators. For moderate conditions described in Appendix A, this finding can be generalized via the following approximation:

$$\frac{\hat{\text{Var}}(\hat{\mu}_{GREG})}{\hat{\text{Var}}(\hat{\mu}_{PSTR})} \approx \frac{1}{\overline{\text{UA}}} \tag{17}$$

where $\overline{\text{UA}} = \frac{\text{UA}_{nonforest} + \text{UA}_{forest}}{2}$ and $\text{UA}_{nonforest} \approx \text{UA}_{forest}$. Thus, under these conditions, the PSTR estimators produce greater precision, but as the UAs simultaneously approach 1.0, the precision for the GREG estimator approaches precision for the PSTR estimator. For the SC-derived forest–nonforest maps, $\text{UA}_{nonforest} \approx \text{UA}_{forest}$ and $\frac{1}{\overline{\text{UA}}} \approx 1.18$ with the result that $\frac{\hat{\text{Var}}(\hat{\mu}_{GREG})}{\hat{\text{Var}}(\hat{\mu}_{PSTR})}$ ranged from 1.00 to 1.27, which indicates general confirmation of the approximation (Tables 1 and 2).

Despite the smaller SEs and greater REs for the PSTR estimators relative to the GREG estimators for the categorical forest–nonforest maps, the smallest SEs and the largest REs over all combinations of maps and estimators were obtained using the continuous probability of forest map data for the SC and SC+GFC maps.

5. Conclusions

Six conclusions were drawn from the study. First, auxiliary information in the form of remote sensing based maps has the potential to substantially increase the precision of forest attribute parameter estimates. Although this result has been reported on multiple previous occasions (McRoberts et al. 2014; Olofsson et al. 2014; Vibrans et al. 2013), failure to have observed this phenomenon would have invalidated the entire study. Second, the wide range of synthetic estimates obtained using the model-assisted estimators documents the inappropriateness of estimating forest area simply by adding the areas of population units (pixels) classified as forest. Third, the two additional maps constructed using the logistic regression model and information from the four local and GFC maps produced the greatest map accuracies. Thus, combining existing maps merits consideration. Fourth, regardless of the combination of map and estimator, estimates of proportion forest area were similar as would be expected when using unbiased or asymptotically unbiased estimators. Fifth, for a categorical response variable whose classes correspond to strata, the PSTR estimators produced greater precision than the model-assisted, generalized regression estimators. However, estimates obtained using the continuous map data, probability of forest, and the generalized regression estimator produced the greatest overall precision. Sixth, the GFC map was the least accurate map and produced the least precise estimates of forest area. However, when used with the PSTR estimators, the forest–nonforest maps

derived from the GFC map still produced relative efficiencies greater than 1.0, indicating that the maps produced greater precision than the SRS estimators. Thus, if local maps are not available or cannot be constructed, then the GFC map merits consideration as a source of auxiliary information for constructing strata for use with PSTR estimators.

The primary contributions of the study to the larger topic area are two-fold. First, the general manner in which a relatively new topic area progresses is via the accumulation of empirical results that are eventually generalized. This is one of only three known reported studies that have used statistically rigorous methods to assess the utility of global maps for national REDD applications, the others being Sannier et al. (2016) and Næsset et al. (2016). Thus, the first contribution of this study is its contribution to an initial body of results from which generalizations will eventually be formulated. Second, the derivation in Appendix A, which is further discussed in Section 4.5, provides a statistical foundation for the observed but previously unexplained finding that when the response and auxiliary variables are categorical with the same classes, the stratified estimator is more precise than the model-assisted regression estimator.

Acknowledgements

The authors thank Fundação de Amparo à Pesquisa e Inovação de Santa Catarina (FAPESC) for supporting the IFFSC and Conselho Nacional de Desenvolvimento Científico e Tecnológico (CNPq) for the research grant awarded to the second author. The authors also thank Stephen V. Stehman, State University of New York, for discussions related to comparisons of the PSTR and model-assisted estimators.

References

Agresti, A. 2007. An introduction to categorical data analysis. Wiley-Interscience, Hoboken, New Jersey.

Aune-Lundberg, L., and Strand, G.-H. 2014. Comparison of variance estimation methods for use with two dimensional systematic sampling of land use/land cover data. Environ. Model. Softw. **61**: 87–97. doi:10.1016/j.envsoft.2014.07.001.

Breidt, F.J., and Opsomer, J.D. 2008. Endogenous post-stratification in surveys: classifying with a sample-fitted model. Ann. Stat. **36**(1): 403–427. doi:10.1214/009053607000000703.

Cochran, W.G. 1977. Sampling techniques. 3rd edition. Wiley, New York.

Cruz, C.B.M., and Vicens, R.S. 2007. Levantamento da Cobertura Vegetal Nativa do Bioma Mata Atlântica. Relatório Final. Rio de Janeiro: IESB/IGEO/UFRJ/UFF.

Dahlke, M., Breidt, F.J., Opsomer, J., and Van Keilegom, I. 2013. Nonparametric endogenous post-stratification. Stat. Sin. **23**: 189–211. doi:10.5705/ss.2011.272.

Fundação SOS Mata Atlântic. 2009. Atlas dos remanescentes florestais da Mata Atlântica, período 2005-2008. Relatório Final. São Paulo: Fundação S.O.S. Mata Atlântica/Instituto Nacional de Pesquisas Espaciais.

Geoambiente Sensoriamento Remoto Ltda. 2008. Projeto de Proteção da Mata Atlântica em Santa Catarina (PPMA/SC). Relatório Técnico do Mapeamento Temático Geral do Estado de Santa Catarina. São José dos Campos.

Global Forest Observations Initiative (GFOI). 2013. Integrating remote-sensing and ground-based observations for estimation of emissions and removals of greenhouse gases in forests. Methods and Guidance from the Global Forest Observations Initiative. Group on Earth Observations, Geneva, Switzerland.

Global Forest Observations Initiative (GFOI). 2015. Module 2: use of global tree cover and change datasets in REDD+ Measuring, Reporting and Verifying (MRV). Available from http://www.gfoi.org/wp-content/uploads/2015/03/MGDModule2_Use-of-Global-Data-Sets.pdf [accessed November 2015].

Gregoire, T.G., and Valentime, H.T. 2008. Sampling strategies for natural resources and the environment. Chapman & Hall/CRC, Boca Raton, Florida.

Hansen, M.C., Potapov, P.V., Moore, R., Hancher, M., Turubanova, S.A., Tyukavina, A., Thau, D., Stehman, S.V., Goetz, S.J., Loveland, T.R., Kommareddy, A., Egorov, A., Chini, L., Justice, C.O., and Townshend, J.R.G. 2013. High-Resolution global maps of 21st-century forest cover change. Science, **342**: 850–853. doi:10.1126/science.1244693.

Jun, C., Ban, Y., and Li, S. 2014. China: open access to Earth land-cover map. Nature, **514**(7523): 434. doi:10.1038/514434c.

Klein, R.M. 1978. Mapa fitogeográfico do estado de Santa Catarina. Itajaí: SUDESUL, FATMA, HBR. (Flora Ilustrada Catarinense, 5).

McRoberts, R.E. 2011. Satellite image-based maps: scientific inference or pretty pictures? Remote Sens. Environ. **115**: 715–724. doi:10.1016/j.rse.2010.10.013.

McRoberts, R.E. 2014. Post-classification approaches to estimating change in forest area using remotely sensed auxiliary data. Remote Sens. Environ. **151**: 149–156. doi:10.1016/j.rse.2013.03.036.

McRoberts, R.E., Wendt, D.G., Nelson, M.D., and Hansen, M.H. 2002. Using a land cover classification based on satellite imagery to improve the precision of forest inventory area estimates. Remote Sens. Environ. **81**: 36–44. doi:10.1016/S0034-4257(01)00330-3.

McRoberts, R.E., Holden, G.R., Nelson, M.D., Liknes, G.C., and Gormanson, D.D. 2005. Using satellite imagery as ancillary data for increasing the precision of estimates for the Forest Inventory and Analysis program of the USDA Forest Service. Can. J. For. Res. **35**(12): 2968–2980. doi:10.1139/x05-222.

McRoberts, R.E., Næsset, E., and Gobakken, T. 2013. Inference for lidar-assisted estimation of forest growing stock volume. Remote Sens. Environ. **128**: 268–275. doi:10.1016/j.rse.2012.10.007.

McRoberts, R.E., Liknes, G.C., and Domke, G.M. 2014. Using a remote sensing-based, percent tree cover map to enhance forest inventory estimation. For. Ecol. Manage. **331**: 12–18. doi:10.1016/j.foreco.2014.07.025.

Næsset, E., Ørka, H.O., Solberg, S., Bollandsås, O.M., Hansen, E.H., Mauya, E., Zahabu, E., Malimbwi, R., Chamuya, N., Olsson, H., and Gobakken, T. 2016. Mapping and estimating forest area and aboveground biomass in miombo woodlands in Tanzania using data from airborne laser scanning, TanDEM-X, RapidEye, and global forest maps: a comparison of estimated precision. Remote Sensing of Environment, **175**: 282–300.

Olofsson, P., Foody, G.M., Stehman, S.V., and Woodcock, C.E. 2013. Making better use of accuracy data in land change studies: Estimating accuracy and area and quantifying uncertainty using stratified estimation. Remote Sens. Environ. **129**: 122–131. doi:10.1016/j.rse.2012.10.031.

Olofsson, P., Foody, G.M., Herold, M., Stehman, S.V., Woodcock, C.E., and Wulder, M.A. 2014. Good practices for estimating area and assessing accuracy of land change. Remote Sens. Environ. **148**: 42–57. doi:10.1016/j.rse.2014.02.015.

Penman, J., Gytarsky, M., Hiraishi, T., Krug, T., Kruger, D., Pipatti, R., Buendia, L., Miwa, K., Ngara, T., Tanabe, K., and Wagner, F. 2003. Good practice guidance for land use, land-use change and forestry. Institute for Global Environmental Strategies, Hayama, Kanagawa Japan. Available from http://www.ipcc-nggip.iges.or.jp [last accessed 15 May 2016].

Potapov, P.V., Dempewolf, J., Talero, Y., Hansen, M.C., Stehman, S.V., Vargas, C., Rojas, E.J., Castillo, D., Mendoza, E., Calderón, A., Giudice, R., Malaga, N., and Zutta, B.R. 2014. National satellite-based humid tropical forest change assessment in Peru in support of REDD+ implementation. Environ. Res. Lett. **9**: 124012. doi:10.1088/1748-9326/9/12/124012.

Sannier, C., McRoberts, R.E., Fichet, L.-V., and Makaga, E.M.K. 2014. Using the regression estimator with Landsat data to estimate proportion forest cover and net proportion deforestation in Gabon. Remote Sens. Environ. **151**: 138–48. doi:10.1016/j.rse.2013.09.015.

Sannier, C., McRoberts, R.E., and Fichet, L.-V. 2016. Suitability of Global Forest Change data to report forest cover estimates at national level in Gabon. Remote Sens. Environ. **173**: 326–338. doi:10.1016/j.rse.2015.10.032.

SAR. 2005. Secretaria de Agricultura e Abastecimento do Estado de Santa Catarina, Inventário Florístico Florestal de Santa Catarina, Relatório do Projeto Piloto, Florianópolis (mimeo).

Särndal, C.-E. 2011. Combined inference in survey sampling. Pakistan Journal of Statistics, **27**(4): 359–370.

Särndal, C.-E., Swensson, B., and Wretman, J. 1992. Model assisted survey sampling. Springer, New York.

Shimada, M., Itoh, T., Motooka, T., Watanabe, M., Shiraishi, T., Thapa, R., and Lucas, R. 2014. New global forest/non-forest maps from ALOS PALSAR data (2007–2010). Remote Sens. Environ. **155**: 13–31. doi:10.1016/j.rse.2014.04.014.

Stehman, S.V. 2009. Sampling designs for accuracy assessment of land cover. Int. J. Remote Sens. **30**: 5243–5272. doi:10.1080/01431160903131000.

Stehman, S.V. 2013. Estimating area from an accuracy assessment error matrix. Remote Sens. Environ. **132**: 202–211. doi:10.1016/j.rse.2013.01.016.

Tipton, J.R., Opsomer, J.D., and Moisen, G.G. 2013. Properties of the endogenous post-stratified estimator using a Random Forest model. Remote Sens. Enviro. **139**: 130–137. doi:10.1016/j.rse.2013.07.035.

Tyukavina, T., Stehman, S.V., Potapov, P.V., Turubanova, S.A., Baccini, A., Goetz, S.J., Laporte, N.T., Houghton, R.A., and Hansen, M.C. 2013. National-scale estimation of gross forest aboveground carbon loss: a case study of the Democratic Republic of the Congo. Environ. Res. Lett. **8**: 044039. doi:10.1088/1748-9326/8/4/044039.

United Nations Framework Convention on Climate Change (UNFCCC). 2006. Decision 16/CMP.1. Available from http://unfccc.int/resource/docs/2005/cmp1/eng/08a03.pdf [accessed 26 February 2015].

Veloso, H.P., Rangel Filho, A.L., and Lima, J.C.A. 1991. Classificação da vegetação brasileira, adaptada a um sistema universal. IBGE, Rio de Janeiro.

Vibrans, A.C., Sevegnani, L., Lingner, D.V., Gasper, A.L., and Sabbagh, S. 2010. Inventário Florístico Florestal de Santa Catarina (IFFSC): aspectos metodológicos e operacionais. Pesquisa Florestal Brasileira, **30**(64): 291–302. doi:10.4336/2010.pfb.30.64.291.

Vibrans, A.C., McRoberts, R.E., Moser, P., and Nicoletti, A.L. 2013. Using satellite image-based maps and ground inventory data to estimate the area of the remaining Atlantic forest in the Brazilian state of Santa Catarina. Remote Sens. Environ. **130**: 87–95. doi:10.1016/j.rse.2012.10.023.

Voigt, C., and Ferreira, F. 2015. The Warsaw Framework for REDD+: implications for national implementation and access to results-based finance. Carbon and Climate Law Review, **9**(2).

Westfall, J.A., Patterson, P.L., and Coulston, J.W. 2011. Post-stratified estimation:

within-strata and total sample size recommendations. Can. J. For. Res. **41**(5): 1130–1139. doi:10.1139/x11-031.

Wolter, K.M. 1984. An investigation of some estimators of variance for systematic sampling. J. Am. Stat. Assoc. **79**(388): 781–790. doi:10.1080/01621459.1984.10477095.

Appendix A

For a forest–nonforest map whose classes are used as strata for stratified estimation of proportion forest using forest–nonforest observations, the error matrix is as depicted in Appendix Table A1. When the Appendix Table A1 cell entries are divided by their corresponding map class marginal totals so that

$$p_{ij} = \frac{n_{ij}}{n_{i\cdot}} \tag{A1}$$

then the error matrix is as depicted in Appendix Table A2. Note that Appendix Table A2 is formulated by dividing the cell entries by the marginal totals, not the total sample size. With this formulation, p_{00} and p_{11} are the user's accuracies, and p_{01} and p_{10} are the corresponding proportional errors of commission.

The generalized regression (GREG) estimators take the forms

$$\hat{\mu}_{\mathrm{GREG}} = \frac{1}{N}\sum_{i=1}^{N}\hat{y}_i - \frac{1}{n}\sum_{i=1}^{n}\varepsilon_i \tag{A2}$$

and

$$\hat{\mathrm{V}}\mathrm{ar}(\hat{\mu}_{\mathrm{GREG}}) = \frac{1}{n(n-1)}\sum_{i=1}^{n}(\varepsilon_i - \bar{\varepsilon})^2 \tag{A3}$$

where N is the population size, $n = n_{0\cdot} + n_{1\cdot} = n_{00} + n_{01} + n_{10} + n_{11}$ is the sample size, $\varepsilon_i = \hat{y}_i - y_i$, and $\bar{\varepsilon} = \frac{1}{n}\sum_{i=1}^{n}\varepsilon_i$ (Särndal et al. 1992). For $\bar{\varepsilon} \approx 0$, the GREG variance estimator can be approximated as

$$\hat{\mathrm{V}}\mathrm{ar}(\hat{\mu}_{\mathrm{GREG}}) = \frac{1}{n(n-1)}\sum_{i=1}^{n}\varepsilon_i^2$$

Further, noting that $\varepsilon_i^2 = (y_i - \hat{y}_i)^2 = \begin{cases} 0 & \text{if } y_i = \hat{y}_i \\ 1 & \text{if } y_i \neq \hat{y}_i \end{cases}$, the GREG variance estimator can be expressed as

$$\hat{\mathrm{V}}\mathrm{ar}(\hat{\mu}_{\mathrm{GREG}}) \approx \frac{n_{01} + n_{10}}{n(n-1)} = \frac{n_{0\cdot}p_{01} + n_{1\cdot}p_{10}}{n(n-1)} \tag{A4}$$

Further noting that $p_{01} = 1 - p_{00}$ and $p_{10} = 1 - p_{11}$, the GREG variance estimator can finally be expressed as

$$\hat{\mathrm{V}}\mathrm{ar}(\hat{\mu}_{\mathrm{GREG}}) \approx \frac{n_{0\cdot}(1 - p_{00}) + n_{1\cdot}(1 - p_{11})}{n(n-1)} \tag{A5}$$

The poststratified (PSTR) estimators are

$$\hat{\mu}_{\mathrm{PSTR}} = \sum_{h=1}^{H} w_h\hat{\mu}_h \tag{A6}$$

and

Appendix Table A1. Error matrix with counts.

	Reference class		
Map class	Nonforest ($y = 0$)	Forest ($y = 1$)	Total
Nonforest ($\hat{y} = 0$)	n_{00}	n_{01}	$n_{0\cdot} = n_{00} + n_{01}$
Forest ($\hat{y} = 1$)	n_{10}	n_{11}	$n_{1\cdot} = n_{10} + n_{11}$

Appendix Table A2. Error matrix with proportions.

	Reference class		
Map class	Nonforest ($y = 0$)	Forest ($y = 1$)	Total
Nonforest ($\hat{y} = 0$)	$p_{00} = \frac{n_{00}}{n_{0\cdot}}$	$p_{01} = \frac{n_{01}}{n_{0\cdot}}$	$n_{0\cdot} = n_{00} + n_{01}$
Forest ($\hat{y} = 1$)	$p_{10} = \frac{n_{10}}{n_{1\cdot}}$	$p_{11} = \frac{n_{11}}{n_{1\cdot}}$	$n_{1\cdot} = n_{10} + n_{11}$

$$\hat{\mathrm{V}}\mathrm{ar}(\hat{\mu}_{\mathrm{PSTR}}) = \sum_{h=1}^{H}\hat{\sigma}_h^2\left(\frac{w_h}{n} + \frac{1 - w_h}{n^2}\right) \tag{A7}$$

where $h = 1, \ldots, H$ indexes the strata; $\hat{\mu}_h$, $\hat{\sigma}_h^2$, n_h, and N_h are the within-stratum sample mean, sample variance, sample size, and population size, respectively; and $w_h = \frac{N_h}{N}$. For equal within-strata sampling intensities and large sample sizes, $w_h \approx \frac{n_{h\cdot}}{n}$ and $\frac{1 - w_h}{n^2} \approx 0$ with the result that

$$\hat{\mathrm{V}}\mathrm{ar}(\hat{\mu}_{\mathrm{PSTR}}) \approx \sum_{h=1}^{H}\left(\frac{n_{h\cdot}}{n^2}\right)\hat{\sigma}_h^2$$

which is the usual stratified variance estimator (Cochran 1977, page 92). Because the response variable follows a Bernoulli distribution, $\hat{\sigma}_0^2 = p_{00}(1 - p_{00})$ and $\hat{\sigma}_1^2 = p_{11}(1 - p_{11})$. Thus

$$\begin{aligned}\hat{\mathrm{V}}\mathrm{ar}(\hat{\mu}_{\mathrm{PSTR}}) &\approx \left(\frac{n_{0\cdot}}{n^2}\right)p_{00}(1 - p_{00}) + \left(\frac{n_{1\cdot}}{n^2}\right)p_{11}(1 - p_{11}) \\ &= \frac{1}{n^2}[n_{0\cdot}p_{00}(1 - p_{00}) + n_{1\cdot}p_{11}(1 - p_{11})]\end{aligned} \tag{A8}$$

The ratio of the two variance estimators is

$$\frac{\hat{\mathrm{V}}\mathrm{ar}(\hat{\mu}_{\mathrm{GREG}})}{\hat{\mathrm{V}}\mathrm{ar}(\hat{\mu}_{\mathrm{PSTR}})} \approx \frac{\frac{1}{n(n-1)}[n_{0\cdot}(1 - p_{00}) + n_{1\cdot}(1 - p_{11})]}{\frac{1}{n^2}[n_{0\cdot}p_{00}(1 - p_{00}) + n_{1\cdot}p_{11}(1 - p_{11})]} \tag{A9}$$

If n is sufficiently large that $\frac{n}{n-1} \approx 1$ and the two user's accuracies $\mathrm{UA}_0 = p_{00}$ and $\mathrm{UA}_1 = p_{11}$, are approximately equal, i.e., $p_{00} \approx p_{11}$, then designating the common user's accuracy as $\overline{\mathrm{UA}} = \frac{\mathrm{UA}_0 + \mathrm{UA}_1}{2} = \frac{p_{00} + p_{11}}{2}$ yields

$$\begin{aligned}\frac{\hat{\mathrm{V}}\mathrm{ar}(\hat{\mu}_{\mathrm{GREG}})}{\hat{\mathrm{V}}\mathrm{ar}(\hat{\mu}_{\mathrm{PSTR}})} &\approx \frac{n[n_{0\cdot}(1 - \overline{\mathrm{UA}}) + n_{1\cdot}(1 - \overline{\mathrm{UA}})]}{(n-1)[n_{0\cdot}\overline{\mathrm{UA}}(1 - \overline{\mathrm{UA}}) + n_{1\cdot}\overline{\mathrm{UA}}(1 - \overline{\mathrm{UA}})]} \\ &= \frac{n(n_{0\cdot} + n_{1\cdot})}{(n-1)\overline{\mathrm{UA}}(n_{0\cdot} + n_{1\cdot})} \approx \frac{1}{\overline{\mathrm{UA}}}\end{aligned} \tag{A10}$$